

# Generation of two types of nonclassical optical states using an optical parametric oscillator with a PPKTP crystal

Meiru Huo,<sup>1</sup> Jiliang Qin,<sup>1</sup> Zhihui Yan,<sup>1,2</sup> Xiaojun Jia,<sup>1,2,a)</sup> and Kunchi Peng<sup>1,2</sup>

<sup>1</sup>State Key Laboratory of Quantum Optics and Quantum Optics Devices, Institute of Opto-Electronics, Shanxi University, Taiyuan 030006, People's Republic of China

<sup>2</sup>Collaborative Innovation Center of Extreme Optics, Shanxi University, Taiyuan 030006, People's Republic of China

(Received 1 August 2016; accepted 12 November 2016; published online 28 November 2016)

As important members of nonclassical states of light, squeezed states and entangled states are basic resources for realizing quantum measurements and constructing quantum information networks. We experimentally demonstrate that the two types of nonclassical optical states can be generated from an optical parametric oscillator (OPO) involving a periodically poled KTiOPO<sub>4</sub> crystal with a domain-inversion period of 51.7 μm, by changing the polarization of the pump laser. When a vertically polarized 671 nm laser is used to pump the OPO, the intra-cavity frequency-down-conversion with type-0 quasi-phase matching is realized and the output optical beam is a quadrature amplitude squeezed state of light at the wavelength of 1342 nm with the fluctuation of quadrature component of 3.17 dB below the quantum noise limit (QNL). If the pump laser is horizontally polarized, the condition of the type-II quasi-phase matching is satisfied and the output optical beam becomes Einstein-Podolsky-Rosen entangled state of light with correlation variances of both quadrature amplitude-sum and quadrature phase-difference of 2.2 dB below the corresponding QNL. Published by AIP Publishing. [<http://dx.doi.org/10.1063/1.4968801>]

In recent years, non classical states of light have been widely applied in quantum information and quantum communication.<sup>1</sup> Squeezed states of light with the quantum noise in one quadrature lower than the standard quantum noise limit (QNL) have been used to quantum key distribution and precision measurements.<sup>2–9</sup> Einstein-Podolsky-Rosen (EPR) entangled states of light, have been utilized in a variety of quantum protocols, such as quantum teleportation, quantum computing, quantum random number generator and quantum metrology, etc.<sup>10–14</sup> Optical parametric oscillator (OPO) is one of the most efficient devices for producing squeezed and EPR entangled states of light, and the quality of the nonclassical states of light from OPO has been continuously improved.<sup>15–24</sup> The entanglement in both the amplitude difference and phase sum quadratures between twin beams from an above threshold OPO was also measured by Villar *et al.*<sup>25</sup> Usually, an OPO involving a nonlinear crystal can only generate a type of nonclassical optical state due to different requirements for phase matching in different nonlinear optical conversions, or both the squeezed noise power of ±45° modes and the correlated noise power of signal and idler beams from a type-II phase matching OPO with a bulk KTiOPO<sub>4</sub> (KTP) crystal can be measured by rotating the polarization of the output beam.<sup>26</sup> With the development of technology of periodic poling, several types of phase matching can be simultaneously realized in a piece of periodic poling crystal. Simultaneous type-0 and type-II spontaneous parametric down-conversions have been realized in a single periodically poled KTiOPO<sub>4</sub> (PPKTP) crystal.<sup>27</sup> Pysher *et al.* even observed three types of phase matching in the process of second harmonic generation of 745 nm.<sup>28</sup> Thus the

periodic poling crystal is possible to be applied in generating exotic entangled states requiring both squeezed state and EPR state for quantum information processing. Here, we present an experimental demonstration of generating two types of non classical optical states from a subthreshold OPO consisting of a PPKTP crystal by changing the polarization of the pump laser. Based on the phase-matching theory in Sellmeier equation, both type-0 and type-II quasi-phase-matching (QPM) for light with the same wavelength in a PPKTP crystal can be implemented,<sup>29–32</sup> in which the nonlinear polarization tensor component  $d_{33}$  for realizing third-order QPM and the nonlinear polarization tensor component  $d_{24}$  for realizing first-order QPM are used,<sup>33</sup> respectively. Due to the poled cycle ( $\Lambda^0$ ) for type-0 QPM is one third of that ( $\Lambda^I$ ) for type-II QPM, both third-order type-0 QPM process and first-order type-II QPM process conditions can be satisfied in the crystal under different operation conditions.<sup>27,34,35</sup> We design and build an OPO containing a PPKTP crystal, with which both single-mode squeezed state and entangled state of light can be produced. When a vertically polarized 671 nm laser is used to pump the OPO, type-0 QPM is achieved and the output optical beam is a single-mode quadrature amplitude squeezed state of light with the quantum fluctuation of  $3.17 \pm 0.14$  dB below the corresponding QNL. If the pump laser is horizontally polarized, the condition of the type-II QPM is satisfied and the output optical beam becomes the EPR entangled state of light with the correlation variances of quadrature amplitude-sum and quadrature phase-difference of  $2.27 \pm 0.16$  dB and  $2.23 \pm 0.15$  dB below the corresponding QNL, respectively.

Generally, the vertically (horizontally) polarized pump laser can produce horizontally (vertically) polarized signal and idler modes in a normal type-I phase matching crystal

<sup>a)</sup>Electronic mail: jiaxj@sxu.edu.cn

via the frequency-down-conversion. However, for a periodically poled crystal, the polarizations of pump, signal, and idler modes can be the same sometimes, which is usually called type-0 phase matching. If a type-I or type-0 phase matching nonlinear crystal is placed in an optical cavity, the polarizations of two parametric down converted optical beams are the same and the output beam usually is a single-mode squeezed state of light.<sup>16,17</sup> When the crystal is operated under the condition of type-II phase matching, the polarizations of the signal and the idler modes will be perpendicular to each other and the two output optical beams separated by a polarization beam splitter (PBS) will constitute a two-mode EPR entangled state of light.<sup>19,24</sup> For any frequency-down-conversion process, the pump, signal and idler modes in an OPO with PPKTP should satisfy QPM conditions, that are,<sup>27,35</sup>

$$\omega_0 = \omega_1 + \omega_2, \quad (1)$$

$$\mathbf{k}_0 = \mathbf{k}_1 + \mathbf{k}_2 + m\mathbf{K}_g, \quad (2)$$

where the subscripts 0, 1, 2 represent the pump, signal and idler modes, respectively.  $\omega_j$  ( $j=0, 1, 2$ ) and  $\mathbf{k}_j$  ( $|\mathbf{k}_j| = \frac{2\pi n_j}{\lambda_j}$ ) are their angular frequency and wave vector in the propagational direction.  $K_g = \frac{2\pi}{\Lambda}$ , is the QPM grating vector,  $\Lambda$  is the poled cycle of the PPKTP crystal which depends on the type of the phase matching. The integer  $m$ , is the QPM order.  $n_j$  and  $\lambda_j$  are the refractive index of the crystal and the wavelength for the corresponding mode, respectively. Eq. (1) indicates that the QPM process satisfies the energy conservation, and Eq. (2) is for the momentum conservation.

The conditions of the phase matching for generating squeezed state and the EPR entangled state are different. For the third order ( $m=3$ ) type-0 QPM process as shown in the left part of Fig. 1, the vertically polarized pump mode produces the vertically polarized signal and idler modes with a degenerate frequency ( $\omega_1 = \omega_2 = \omega_0/2$ ) in an OPO via a frequency-down-conversion process. The output signal and idler modes constitute a single-mode squeezed state of light. In this case, Eq. (2) is expressed as

$$\mathbf{k}_0^z = \mathbf{k}_1^z + \mathbf{k}_2^z + 3\mathbf{K}_g^0, \quad (3)$$

where,  $\mathbf{K}_g^0$  is the grating vector for type-0 QPM, and the refractive indices corresponding to  $z$  axis of PPKTP crystal should be used to calculate the wave vector magnitude ( $|\mathbf{k}_j^z| = \frac{2\pi n_j^z}{\lambda_j}$  ( $j=0, 1, 2$ )) because all optical modes in this process are vertically polarized.

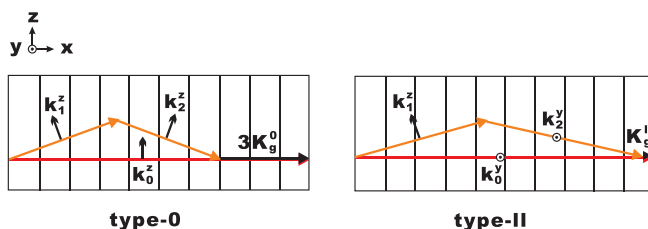


FIG. 1. Wave vector diagram in the  $x$ - $z$  plane of PPKTP crystal for type-0 and type-II QPM processes.

If a horizontally polarized laser is used as the pump mode, the type-II QPM parametric down conversion will occur in the OPO and in this case, the vertically polarized signal mode and the horizontally polarized idler mode with a degenerate frequency will be produced. The condition in the process of the first order ( $m=1$ ) type-II QPM becomes

$$\mathbf{k}_0^y = \mathbf{k}_1^z + \mathbf{k}_2^y + \mathbf{K}_g^{II}, \quad (4)$$

where  $\mathbf{K}_g^{II}$  is the grating vector for type-II QPM,  $|\mathbf{k}_0^y| = \frac{2\pi n_0^y}{\lambda_0}$  and  $|\mathbf{k}_2^y| = \frac{2\pi n_2^y}{\lambda_2}$  correspond to wave vectors of the pump mode and idler mode with the polarization along the  $y$  axis of PPKTP crystal, and  $|\mathbf{k}_1^z| = \frac{2\pi n_1^z}{\lambda_1}$  is the wave vector of the signal mode with the polarization along the  $z$  axis. Since  $n_j^y \neq n_j^z$  for a PPKTP crystal, Eqs. (3) and (4) stand for different QPM conditions.

The experimental schematic for the generation of nonclassical states of light is shown in Fig. 2. A dual-wavelength (671 nm and 1342 nm) Nd:YVO<sub>4</sub>/LBO laser (Yuguang Company) is used as the laser source, the output powers of which are 850 mW at a wavelength of 1342 nm and 2.8 W at a wavelength of 671 nm.<sup>36</sup> F-P cavity is used to monitor the single-frequency operating of the laser with a photoelectric detector (PD1). The two lasers at 671 nm and 1342 nm are separated by a dichroic beam splitter (DBS) and each of them passes through a mode-cleaner (MCR and MCI), respectively, for implementing the spatio-temporal filtering and increasing the intensity stability, the finesse of MCR and MCI are 400 at 671 nm and 300 at 1342 nm, respectively. The piezoelectric ceramics (PZT1-3) are mounted to a concave mirror of F-P cavity and mode-cleaners, respectively, to sweep or lock the length of optical cavities. The OPO cavity consists of a pair of concave mirrors, whose diameters is 10 mm and the curvature radius is 50 mm. A PPKTP crystal with a size of  $1 \times 2 \times 12$  mm<sup>3</sup> is placed in a copper oven above the two cascaded thermoelectric coolers to control its temperature. The separation between two cavity mirrors is 104 mm and the waist of 1342 nm infrared mode is about 46  $\mu$ m in the center of the crystal. The input mirror is coated of film with reflectivity  $R > 99.8\%$  at 1342 nm and transmission  $T = 95.2\%$  at 671 nm, and the output mirror is coated with transmission  $T = 2\%$  at 1342 nm and reflectivity  $R > 99.9\%$  at 671 nm. The 5 mW infrared optical beam (the seed mode) injected into the OPO cavity is modulated by an EOM (Electro-optic modulator) to generate an error signal, and this signal is fed back to PZT4 mounted on the output mirror of OPO for locking the length of the OPO to resonate with the signal and idler beams via PDH sideband frequency stabilization technique.<sup>37</sup> In our experiment, the match of the pump mode to the OPO cavity should be finished first. We substitute an input mirror of OPO with a temporal concave mirror with the same curvature radius (50 mm) but coated with a certain reflectivity for the pump mode ( $R = 97\%$  for 671 nm in our experiment). In this condition, the finesse of the OPO cavity for the pump mode is more than 100 and then we place a lens with the focal length of 250 mm in optical path of the pump light to complete the mode-matching. Then we replace the temporal mirror by the

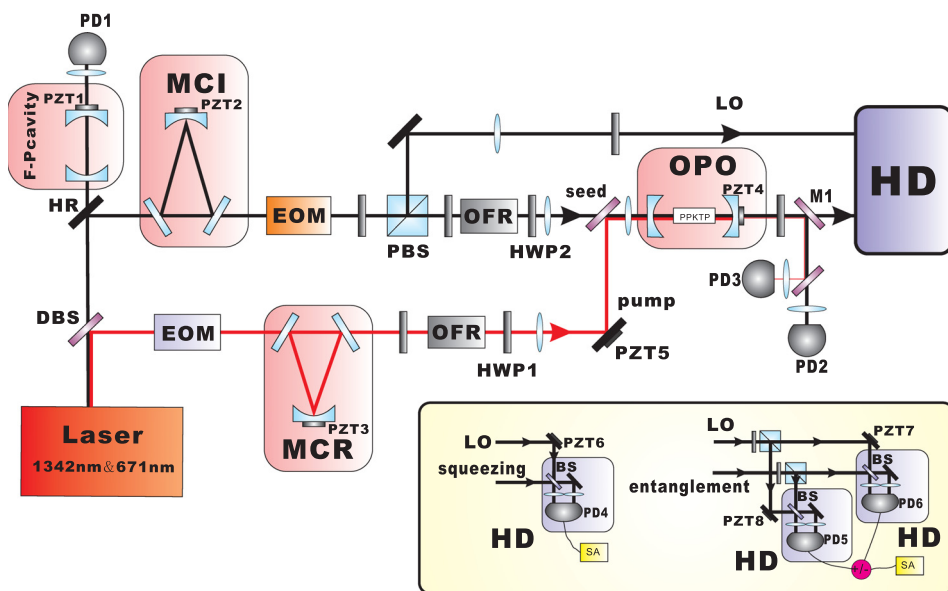


FIG. 2. Experimental setup. Laser: Nd:YVO<sub>4</sub>/LBO; MCR: mode-cleaner for red light beam; MCI: mode-cleaner for infrared light beam; OPO: optical parametric oscillator; HD: homodyne detection; DBS: dichroic beam splitter; EOM: electro-optical modulator; HWP1,2: half-wave plate; OFR: optical Faraday rotator; PBS: polarization beam splitter; M1: mirror with high transmission at 671 nm and high reflectivity at 1342 nm (the same as DBS); BS: 50:50 beam splitter; PD1-6: photoelectric detector; PZT1-8: piezoelectric ceramic; SA: spectrum analyzer. Inset: the detection system of both single-mode quadrature amplitude squeezed state and bipartite EPR entangled state of light.

experimental input coupler again. In the process of experiment, we can also check the mode matching of the pump mode by observing the classical gain of OPO. Once the mode matching of pump beam becomes worse, the classical gain will reduce very quickly. The phase difference between the pump laser and the seed mode is maintained at  $(2k + 1)\pi$  ( $k$  is an integer) with PZT5. Finally, the output beam from OPO and the local oscillator (LO) passing through MCI are sent to the detection system for the measurement of noise power.

When the polarization of both pump and seed beams is rotated to the vertical direction by the half-wave plates, HWP1 and HWP2, the OPO is operated at type-0 QPM condition to generate the single mode quadrature amplitude squeezed state of light. The measured threshold pump power of the OPO is 212 mW. Under the pump power of 150 mW and slowly adjusting the temperature of PPKTP crystal, the optimal parametric transformation is realized at 133.3 °C, and the highest squeezing of the output light with power of 25  $\mu$ W is obtained. The detection system of the squeezed light is shown in the insert of Fig. 2, which includes a 50:50 beam splitter and a two-photodiode balanced homodyne detector (PD4). The photodiodes used are FD500W (Fermionics Opto-Technology company), whose quantum efficiency is 90% at a wavelength of 1342 nm. The power of local oscillator (LO) beam is 15 mW, and the interference visibility between the LO beam and the signal light is 98.7%. The phase difference between the LO beam and the squeezed state is locked to  $k\pi$  ( $k$  is an integer), then the noise power of the quadrature amplitude of the squeezed light is recorded by a spectrum analyzer (SA) connecting with alternating current (AC) output of the PD4. Fig. 3 indicates the noise power of the quadrature amplitude squeezed state of light, where trace (ii) is the noise power of the quadrature amplitude squeezed state and trace (i) is the corresponding QNL, which is measured by blocking the output beam from OPO. It can be seen that the noise power of the squeezed state is  $3.17 \pm 0.14$  dB below the corresponding QNL at the side band of 3 MHz. The resolution bandwidth (RBW) and the video bandwidth (VBW) of SA are set at 100 kHz and 300 Hz, respectively.

If the polarization of the pump laser is rotated to the horizontal direction by HWP1 and the polarization of the seed beam is adjusted to 45° relative to  $y$  axis of the PPKTP crystal by HWP2, the signal and idler modes in the PPKTP have a perpendicular polarization, and the OPO is operated at type-II QPM condition. In this case, the simultaneous resonance of the signal and idler beams in OPO is realized by tuning the temperature of the PPKTP crystal, and the output signal and idler optical modes constitute an EPR entangled state of light.<sup>19</sup> When the power of pump laser is 280 mW which is below the threshold (420 mW) and the temperature of PPKTP crystal is controlled to 116 °C, the best entangled state of light is obtained. In our experiment, the phase difference between the pump laser and the seed mode is maintained at  $(2k + 1)\pi$  ( $k$  is an integer), i.e., the OPO works in de-amplification condition, and the correlation style of the output EPR entangled beams is the correlations of the amplitude sum and the phase difference.<sup>24</sup> The measured power of the output beam from the OPO is 30  $\mu$ W in this condition.

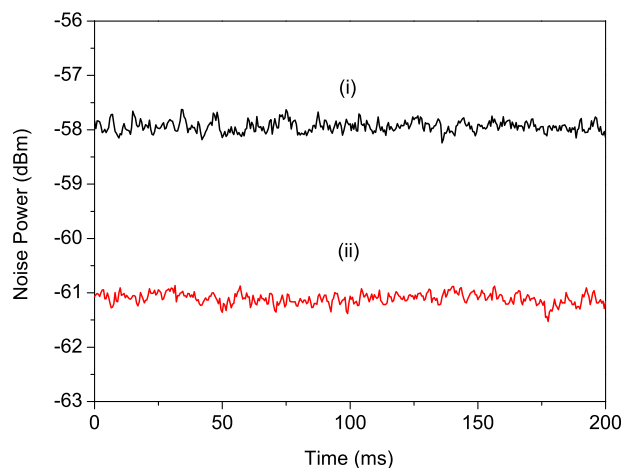


FIG. 3. Measured result of squeezed state of light. The trace (i) is corresponding QNL and trace (ii) is noise power of quadrature amplitude squeezed state. The analysis frequency is 3 MHz, and noise power of quadrature amplitude squeezed state is  $3.17 \pm 0.14$  dB lower than the corresponding QNL. RBW and VBW of SA are 100 kHz and 300 Hz, respectively.



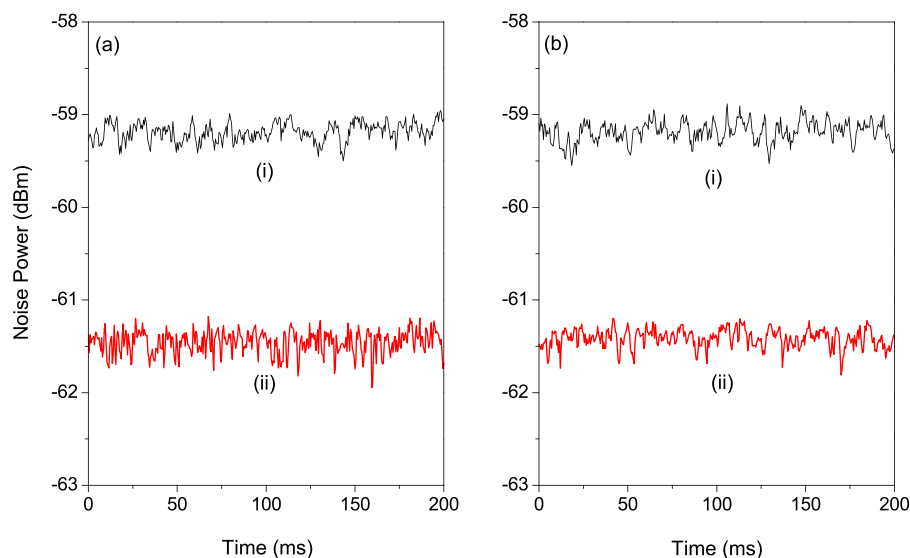


FIG. 4. Measured result of correlation variance for EPR entangled state of light. The trace (i) is corresponding QNL and trace (ii) is correlation variance noise power of quadrature entangled states of light. (a) Correlation variance of quadrature amplitude-sum, which is  $2.27 \pm 0.16$  dB below the corresponding QNL, (b) correlation variance of quadrature phase-difference, which is  $2.23 \pm 0.15$  dB below the corresponding QNL. RBW and VBW of SA are still 100 kHz and 300 Hz.

The detection system for the EPR entangled state is also given in the inset of Fig. 2, which includes two pieces of 50:50 beam splitters and two pairs of two-photodiode balanced homodyne detectors (PD5, 6). The EPR entangled state is separated into two orthogonally polarized optical beams by a PBS and each of them is coupled with a LO beam with the interference visibility of 98.5%. The powers of LO beam in each homodyne detection system are 6 mW and the phase difference of signal (idler) beam and LO beam is locked to  $k\pi$  and  $(k + 1/2)\pi$  ( $k$  is an integer) to measure the noise power of the quadrature amplitude and quadrature phase components of output signal and idler, respectively. Then plus and minus combiners (ZSC-2-1 and ZSCJ-2-1 from Mini-circuits Company) are applied for AC outputs of PD5, 6 to obtain the amplitude-sum and the phase-difference correlation variances between the two EPR entangled optical beams, which are recorded by the SA as shown in Fig. 4. The parameters of SA are the same as those used in Fig. 3. The traces (ii) are correlation variances for amplitude-sum (Fig. 4(a)) and phase-difference (Fig. 4(b)), respectively. The traces (i) are the corresponding QNL which are also measured by blocking the output of the OPO. It is obvious that the correlation variances of amplitude-sum and phase-difference are  $2.27 \pm 0.16$  dB and  $2.23 \pm 0.15$  dB below the corresponding QNL, respectively.

In a summary, we experimentally demonstrate that an OPO consisting of a PPKTP crystal with a domain-inversion period of  $51.7 \mu\text{m}$  can be operated at two situations of type-I and type-II QPM by controlling the polarization of pump light and adjusting the temperature of PPKTP crystal. Thus, two types of nonclassical optical states can be produced by the system. If the transmissivity of the OPO is increased further, the quality of the generated non-classical states of light will be possibly improved.<sup>17,24</sup> Moreover, when the crystal is specially designed and a  $45^\circ$  polarized laser at the wavelength of 671 nm is used as the pump laser of the OPO, both squeezed state and EPR entangled state will possibly be obtained at the same time. We believe that the presented system is able to be developed as a practical and versatile device for the generation of different types of nonclassical light.

We acknowledge the support from the Key Project of the Ministry of Science and Technology of China (Grant No. 2016YFA0301402), the Natural Science Foundation of China (Grant Nos. 11322440, 11474190, 11304190), FOK YING TUNG Education Foundation, Natural Science Foundation of Shanxi Province (Grant No. 2014021001), the Program for Sanjin Scholars of Shanxi Province.

- <sup>1</sup>S. L. Braunstein and P. van Loock, *Rev. Mod. Phys.* **77**, 513 (2005).
- <sup>2</sup>N. J. Cerf, M. Levy, and G. V. Assche, *Phys. Rev. A* **63**, 052311 (2001).
- <sup>3</sup>R. G. Patron and N. J. Cerf, *Phys. Rev. Lett.* **102**, 130501 (2009).
- <sup>4</sup>The LIGO Scientific Collaboration, *Nat. Photonics* **7**, 613 (2013).
- <sup>5</sup>N. Treps, N. Grosse, W. P. Bowen, C. Fabre, H. A. Bachor, and P. K. Lam, *Science* **301**, 940 (2003).
- <sup>6</sup>W. F. Li, J. J. Du, R. J. Wen, G. Li, and T. C. Zhang, *J. Appl. Phys.* **115**, 123106 (2014).
- <sup>7</sup>H. X. Sun, K. Liu, Z. L. Liu, P. L. Guo, J. X. Zhang, and J. R. Gao, *Appl. Phys. Lett.* **104**, 121908 (2014).
- <sup>8</sup>H. Yonezawa, D. Nakane, T. A. Wheatley, K. Iwasawa, S. Takeda, H. Arao, K. Ohki, K. Tsumura, D. W. Berry, and T. C. Ralph *et al.*, *Science* **337**, 1514 (2012).
- <sup>9</sup>A. Berni, T. Gehring, B. M. Nielsen, V. Handchen, M. G. A. Paris, and U. L. Anderson, *Nat. Photonics* **9**, 577 (2015).
- <sup>10</sup>A. Furusawa, J. L. Sorensen, S. L. Braunstein, C. A. Fuchs, H. J. Kimble, and E. S. Polzik, *Science* **282**, 706 (1998).
- <sup>11</sup>A. K. Ekert, *Phys. Rev. Lett.* **67**, 661 (1991).
- <sup>12</sup>J. I. Cirac, A. K. Ekert, S. F. Huelga, and C. Macchiavello, *Phys. Rev. A* **59**, 4249 (1999).
- <sup>13</sup>X. L. Su, S. H. Hao, X. W. Deng, L. Y. Ma, M. H. Wang, X. J. Jia, C. D. Xie, and K. C. Peng, *Nat. Commun.* **4**, 2828 (2013).
- <sup>14</sup>T. Loughi, J. B. Brask, C. C. W. Lim, Q. Lavigne, J. Bowles, A. Martin, H. Zbinden, and N. Brunner, *Phys. Rev. Lett.* **114**, 150501 (2015).
- <sup>15</sup>L. A. Wu, H. J. Kimble, J. L. Hall, and H. F. Wu, *Phys. Rev. Lett.* **57**, 2520 (1986).
- <sup>16</sup>Y. Takeno, M. Yukawa, H. Yonezawa, and A. Furusawa, *Opt. Express* **15**, 4321 (2007).
- <sup>17</sup>T. Eberle, S. Steinlechner, J. Bauchrowitz, V. Handchen, H. Vahlbruch, M. Mehmet, H. Muller-Ebhardt, and R. Schnabel, *Phys. Rev. Lett.* **104**, 251102 (2010).
- <sup>18</sup>H. Vahlbruch, M. Mehmet, K. Danzmann, and R. Schnabel, *Phys. Rev. Lett.* **117**, 110801 (2016).
- <sup>19</sup>Z. Y. Ou, S. F. Pereira, H. J. Kimble, and K. C. Peng, *Phys. Rev. Lett.* **68**, 3663 (1992).
- <sup>20</sup>W. P. Bowen, R. Schnabel, P. K. Lam, and T. C. Ralph, *Phys. Rev. A* **69**, 012304 (2004).
- <sup>21</sup>J. Laurat, T. Coudreau, G. Keller, N. Treps, and C. Fabre, *Phys. Rev. A* **70**, 042315 (2004).
- <sup>22</sup>N. Takei, H. Yonezawa, T. Aoki, and A. Furusawa, *Phys. Rev. Lett.* **94**, 220502 (2005).

- <sup>23</sup>Y. Wang, H. Shen, X. L. Jin, X. L. Su, C. D. Xie, and K. C. Peng, *Opt. Express* **18**, 6149 (2010).
- <sup>24</sup>Y. Y. Zhou, X. J. Jia, F. Li, C. D. Xie, and K. C. Peng, *Opt. Express* **23**, 4952 (2015).
- <sup>25</sup>A. S. Villar, L. S. Cruz, K. N. Casemiro, M. Martinelli, and P. Nussenzveig, *Phys. Rev. Lett.* **95**, 243603 (2005).
- <sup>26</sup>Z. Y. Ou, S. F. Pereira, and H. J. Kimble, *Appl. Phys. B* **55**, 265 (1992).
- <sup>27</sup>H. J. Lee, H. Kim, M. Cha, and H. S. Moon, *Appl. Phys. B* **108**, 585 (2012).
- <sup>28</sup>M. Pysher, A. Bahabad, P. Peng, A. Arie, and O. Pfister, *Opt. Lett.* **35**, 565 (2010).
- <sup>29</sup>T. Y. Fan, C. E. Huang, B. Q. Hu, R. C. Eckardt, Y. X. Fan, R. L. Byer, and R. S. Feigelson, *Appl. Opt.* **26**, 2390 (1987).
- <sup>30</sup>F. König and F. N. C. Wong, *Appl. Phys. Lett.* **84**, 1644 (2004).
- <sup>31</sup>K. Fradkin, A. Arie, A. Skliar, and G. Rosenman, *Appl. Phys. Lett.* **74**, 914 (1999).
- <sup>32</sup>W. Wiechmann, S. Kubota, T. Fukui, and H. Masuda, *Opt. Lett.* **18**, 1208 (1993).
- <sup>33</sup>H. Vanherzeele and J. D. Bierlein, *Opt. Lett.* **17**, 982 (1992).
- <sup>34</sup>T. Ellenbogen, A. Arie, and S. M. Seltiel, *Opt. Lett.* **32**, 262 (2007).
- <sup>35</sup>J. Chen, A. J. Pearlman, A. Ling, J. Fan, and A. Migdall, *Opt. Express* **17**, 6727 (2009).
- <sup>36</sup>Y. H. Zheng, Y. J. Wang, C. D. Xie, and K. C. Peng, *IEEE J. Quantum Electron.* **48**, 67 (2012).
- <sup>37</sup>R. W. P. Drever, J. L. Hall, F. V. Kowalski, J. Hough, G. M. Ford, A. J. Munley, and H. Ward, *Appl. Phys. B* **31**, 97 (1983).